JOURNAL OF GEOPHYSICAL RESEARCH, VOL. 95, NO. A4, PAGES 4027–4038, APRIL 1, 1990

The Equilibrium of a Conducting Body Embedded in a Flowing Plasma

ANDREW N. WRIGHT AND STEVEN J. SCHWARTZ

Astronomy Unit, School of Mathematical Sciences, Queen Mary and Westfield College, London, England

A conducting body embedded in a magnetized plasma flow may interact with the medium in a variety of ways. Within a MHD description, it is well known that the currents induced within the satellite can be closed in the plasma by standing Alfvén waves attached to it. However, we show that such a simple model (when viewed in the massive satellite rest frame) cannot satisfy continuity of mass, momentum or energy fluxes. The imbalance is due to the neglect of other plasma disturbances, i.e., the fast and slow magnetosonic modes. In this paper we introduce a slow magnetosonic wake and find that a suitable solution can redress the balance demanded by continuity to a large extent. The full solution, including the fast magnetosonic wave, remains an outstanding problem. Our principal conclusion is that it is not possible for a conducting body to excite a purely Alfvénic disturbance; there must be other plasma waves present too.

1. INTRODUCTION

The behaviour of large, electrically conducting bodies embedded in a flowing plasma has received attention for nearly two and a half decades. Some of the earliest work was by *Drell et al.* [1965], who tried to explain the anomalous drag experienced by the Echo 1 satellite. They introduced the important concept of 'Alfvén wings', which are standing Alfvén waves attached to the satellite. As pointed out by Drell et al., the electric current induced within the conductor is closed in the plasma via the characteristic-aligned Alfvénic current. The continuity of current is one of the most appealing physical arguments for the existence of Alfvén waves (or a similar agent) connected to a conductor embedded in a plasma flow. In their paper, Drell et al. also considered the properties of Alfvén waves on other physical grounds - namely conservation of energy. They predicted a simple balance between the decreasing kinetic energy of the conductor, and the Poynting flux of the Alfvén waves. Some caution is needed when discussing an energy balance because the description is frame-dependent - unlike current continuity. In addition, if there are non-Alfvénic disturbances within the plasma some of the energy is not taken into account. The following year detailed calculations of the drag on long cylindrical satellites were performed [*Chu and Gross*, 1966]. Much the same picture as before was described, except for a couple of points: The authors admitted the possibility of a non-Alfvénic wake, and also expressed the change in the satellite's kinetic energy in terms of the Lorentz force it experienced.

Goldreich and Lynden-Bell [1969] suggested that the Jovian satellite Io would have a good electrical conductivity, and anticipated a similar current system to that described previously. Following their work attention turned from the behaviour of artificial satellites to natural ones, most notably Io. Several studies of the Alfvén waves near Io have been made [*Goertz and Deift*, 1973; *Neubauer*, 1980; *Southwood et al.*, 1980; *Wright and Southwood*, 1987], and there is excellent agreement with observations from Voyager 1 [*Acuña et al.*, 1981; *Belcher et al.*, 1981; *Barnett*, 1986]. These models have concentrated upon the current carrying properties of Alfvén waves and the expected field and flow perturbations. *Wright and Southwood* [1987] also described the perpendicular current system required to produce the flow perturbation. Some of the most recent work has considered non-Alfvénic disturbances near Io: *Wolf-Gladrow et al.* [1987] modeled the detailed current flow around the satellite, and *Linker et al.* [1988] have found evidence of slow magnetosonic mode perturbations in the wake.

Over the past few years interest in artificial satellites has resumed - mainly due to the Space Shuttle and the possibility of active experiments such as the Tethered Satellite System (TSS). Most studies calculate the wave field in terms of Fourier components, match the current flowing in the conductor to the total wave field and evaluate the radiated power for a variety of different systems, geometries and approximations [*Belcastro et al.*, 1982; *Rasmussen et al.*, 1985; *Barnett and Olbert*, 1986; *Dobrowolny and Veltri*, 1986; *Wright*, 1987; *Hastings et al.*, 1988; *Estes*, 1988; *Rasmussen and Banks*, 1988]. *Barnett and Olbert* [1986] and *Hastings et al.* [1988] do not restrict themselves to the Alfvén mode and consider higher frequency waves. These studies are in general, but not perfect, agreement (see Appendix B).

For the remainder of this paper we shall concentrate upon the three low frequency MHD modes: The Alfvén (sometimes called 'intermediate' or 'shear') mode, the fast (or 'compressional') magnetosonic mode, and the slow magnetosonic mode. For brevity, we shall refer to these waves as simply Alfvén, fast and slow modes, respectively. (See, for example, page 188 of *Boyd and Sanderson* [1969] for a comprehensive review of existing nomenclature.) In the cold plasma limit, the Alfvén mode is sometimes termed 'slow', but we shall avoid this confusing terminology here.

In this paper we restrict our analysis to the low frequency MHD disturbances excited by a satellite. We concentrate primarily upon the Alfvén and slow mode wave-trains. These modes are guided by the background magnetic field, thus preserving their amplitudes at large distances from the satellite. Accordingly they are easier to model, and probably more readily identified in data than the more isotropic fast mode. We have succeeded in considering the slow mode in combination with the previously studied Alfvén mode.

Paper number 89JA03696.
0148-0227/90/89JA-03696$05.00

However a complete solution of the problem must include the effects of the fast mode as well as being fully nonlinear. Although the Alfvén wave train solution we employ is fully nonlinear, our treatment of the conservation laws is only to second order in the Alfvén wave amplitude. Moreover, our slow mode solution makes first order contributions to these laws, and a linear treatment of this mode suffices for the time being. Most of our calculations are performed in the satellite rest frame. We employ the 'massive' satellite approximation, i.e. the satellite is able to supply momentum without acquiring an appreciable velocity of its own. This allows us to treat the plasma disturbances as being steady in time. The behaviour of the satellite kinetics and energetics is easy to describe in this limit, and is the subject of §2. By assuming that all of the current in the satellite is closed in Alfvén waves, we can predict the Alfvén wave field. Given this information it is possible to see if the conductor and the Alfvén waves satisfy continuity of mass, momentum and energy flux. In §3 we perform this calculation by constructing a large imaginary box around the satellite and comparing the net flux in or out of the box with the sources or sinks contained within it. Calculations show it is inevitable that the simple Alfvén wave/conductor system will violate all three continuity equations. Thus we conclude that there must be other disturbances present in the plasma. This is borne out in a recent simulation by *Linker et al.* [1988], who found a standing slow mode wave attached to the satellite, in addition to the Alfvén wave. The slow mode helps to restore equilibrium downstream of the satellite. We estimate the contribution of the slow mode to the continuity equations by using a simple model. We find (in §4) that the slow mode serves, to a large degree, to redress the balance required by continuity. The remaining discrepancy can be accounted for as arising from simplifications and the neglect of the fast mode, as is discussed in §5. In Appendix A we consider the satellite behaviour in the plasma rest frame, and also when the 'massive' limit is not satisfied. Appendix B and C are devoted to the modeling of the Alfvén and slow modes, respectively. Our main conclusion is that it is not possible for a conducting body to excite solely Alfvén waves. There must also be other MHD disturbances, and we are able to estimate the amplitude of the slow mode component.

2. SATELLITE KINETICS AND ENERGETICS

Consider a conducting body embedded in a steady, flowing magnetoplasma. We shall assume that the background plasma velocity and uniform magnetic field are mutually perpendicular. The background convection electric field experienced by the conductor gives rise to an induced electric field that is equal to the perturbation Alfvénic electric field. The amplitude of the Alfvén wave can be determined by requiring that the perturbation electric field allow the same current flow in the satellite as that carried away by the waves [*Neubauer*, 1980; *Southwood et al.*, 1980; *Wright and Southwood*, 1987]. The perturbed quantities, eg. the velocity field $\mathbf{u}$ associated with each wave mode, are not uniform throughout the perturbed region. We shall characterize the amplitue of the perturbation in two ways. First, for each component u_i of $\mathbf{u}$, we denote the extreme value by $\tilde{u}_i$ - which may be positive or negative. Second, the maximum magnitude of the vector $\mathbf{u}$ is denoted by $\tilde{u}$. In this fashion it is possible to express the strength of the Alfvénic velocity perturbation in terms of a dimensionless parameter (ε) times the background flow speed (V_c), i.e. $\tilde{u} = \varepsilon V_c$. The strength of the Alfvén wave (ε) is governed by background quantities, (e.g. equation (29) of *Wright and Southwood* [1987])

$$\varepsilon = \frac{\Sigma_s}{2\Sigma_A + \Sigma_s} \tag{1}$$

Σ_s and Σ_A are the conductances of the satellite, and of the medium to Alfvén waves, respectively. If these conductances are not known with sufficient accuracy, one could regard ε as a free parameter to be determined (along with the amplitudes of the other modes) by the conservation equations given in §3. The factor of two in the denominator of equation (1) is due to the fact that there are two Alfvén waves attached to the satellite. Note that ε varies between 0, for an insulator, to 1 for a perfect conductor. For simplicity we shall idealize the shape of the conductor to a block of dimensions $L_1 \times L_1 \times L_2$, where L_2 is the dimension along the background convection electric field, i.e. perpendicular to $\mathbf{B}_0$ and $\mathbf{V}_c$ (the $\hat{\alpha}$ direction in Figure 1*a*). The effective volume integrated current flowing within the conductor ($\mathbf{I}_s$) can be determined using Ampère's law $I_s \approx L_1\tilde{b}/\mu_0$ - we

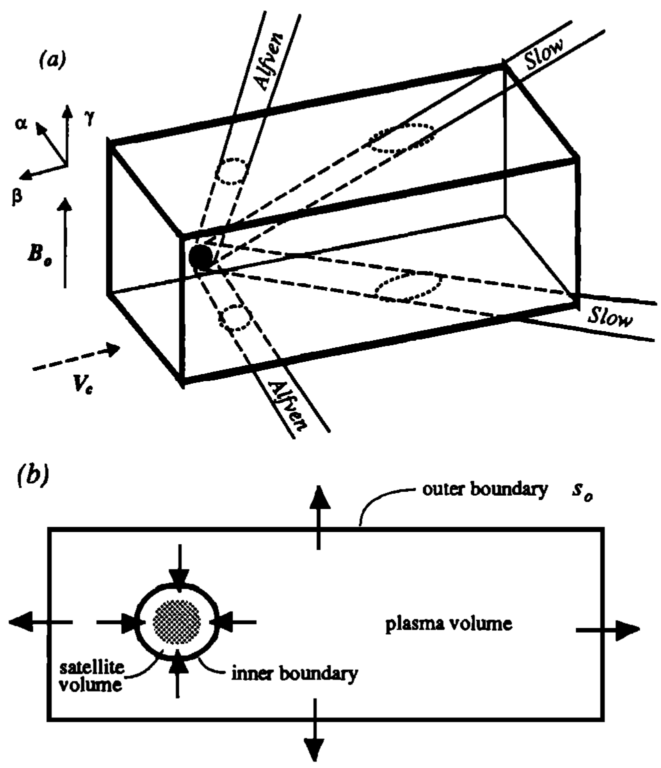

Fig. 1. The massive conductor lies inside the large imaginary box. (*a*) The Alfvén and slow mode waves are both guided along the background magnetic field direction, and form four standing wave-trains in this frame of reference. The box is chosen in such a way that all the wave-trains exit either through the top or bottom face of the box. The orientation of the coordinate system (α, β, γ) is also shown, as are the directions of the background plasma convection velocity ($\mathbf{V}_c$) and magnetic field ($\mathbf{B}_0$). (*b*) The conductor and large box are shown schematically. The plasma within the box has two boundary surfaces. The 'outer' one (refered to as s_0) is the surface of the box, and the 'inner' one sheaths the volume occupied by the satellite. The plasma we are interested in occupies the space between these two surfaces. The direction of outward (positive) fluxes from the plasma volume are shown by the arrows.

have introduced a rough factor of a half since $\tilde{b}$ represents the peak magnetic field perturbation of the Alfvén wave, not the volume-weighted mean one. Let the satellite have mass m_s and move with velocity $\mathbf{V}_s$ in our reference frame. If the background field is $\mathbf{B}_0$, then the satellite momentum ($\mathbf{P}_s$) is governed by

$$\frac{d\mathbf{P}_s}{dt} = m_s \frac{d\mathbf{V}_s}{dt} \equiv L_2 \mathbf{I}_s \wedge \mathbf{B}_0 \tag{2}$$

while the satellite kinetic energy (κ) evolves according to

$$\frac{d\kappa}{dt} = \frac{\mathbf{P}_s}{m_s} \cdot \frac{d\mathbf{P}_s}{dt} \equiv L_2 \mathbf{V}_s \cdot \mathbf{I}_s \wedge \mathbf{B}_0 \tag{3}$$

Using equation (2) we can define what is meant by the 'massive', or 'infinite mass' limit: The relevant MHD time scale may be taken as the time taken for plasma to convect across the satellite, ($\Delta t = L_1/V_c$). Here $\mathbf{V}_c$ is the relative plasma convection velocity. Since L_2, $\mathbf{I}_s$ and $\mathbf{B}_0$ are all well behaved finite quantities, equation (2) tells us that as $m_s \to \infty, d\mathbf{V}_s/dt \to 0$. Put more precisely, we require that the change in V_s/V_c on the MHD time scale Δt be very much less than unity. This is satisfied when

$$m_s \gg \frac{L_1 L_2 B_0 I_s}{V_c^2} \tag{4}$$

and means that the satellite can be treated as a steady source of waves on the time scale that MHD waves are radiated on. It is interesting to see that in this limit (and when viewed from the frame in which $\mathbf{V}_s(t=0)=0$) the satellite momentum increases linearly with time $\mathbf{P}_s(t) = \mathbf{P}_s(0) + L_2 \mathbf{I}_s \wedge \mathbf{B}_0 t$, while the kinetic energy remains zero for all time. The latter result is due to the Lorentz force on the satellite not doing any work on the body in this choice of reference frame ($\mathbf{V}_s(t) \approx \mathbf{V}_s(0) = 0$) - see equation (3). We shall restrict ourselves to the massive satellite limit and the conductor's rest frame for the remainder of the paper, although alternative choices are discussed in Appendix A for completeness. Now let us consider the effect of the satellite upon mass, momentum and energy fluxes in the limit described above. To do this we shall model the slow and Alfvén wave-trains as shown in Figure 1*a*. Due to the differences in Alfvén and slow mode phase velocities, these wave-trains are inclined at different angles with respect to $\mathbf{B}_0$ as shown in the figure. The conductor is inside a large box containing plasma. In Figure 1*b* the system is shown in a schematic fashion. There are two surfaces bounding the plasma; one is the surface of the large box, and the other is an imaginary envelope that sheaths the conductor. The approach adopted throughout this paper is to consider fluxes across these surfaces. In equilibrium the total outward flux from the plasma (of any conserved quantity) must be zero, as there are no sources or sinks in the volume between the two surfaces that is occupied by plasma. (Note that the conductor may act as a source or sink, but this lies on the opposite side of the inner boundary to the plasma.)

Below we calculate the fluxes across the inner boundary surrounding the satellite. This is done most easily by using Gauss' theorem which tells us that the flux integrated over this inner surface is equal to the sum of sources and sinks inside the volume occupied by the conductor. For example, if the system is in equilibrium, and the satellite is a net sink of energy, then there must be a net energy flux out of the plasma volume and into the conductor's volume. In the next section we estimate the fluxes across the outer boundary due to plasma waves. Continuity requires that the sum of fluxes across these two boundaries be zero. We shall use the sign convention that fluxes out of the plasma volume are positive, hence if the satellite acts as a sink it is associated with a positive flux. (Fluxes directed into the plasma volume and satellite sources are negative.) Now let's calculate the fluxes across the inner boundary, starting with the mass flux.

Mass Flux

The simplified model of plasma absorption that is adopted here assumes that a particle is captured by the satellite if its trajectory is coincident with the surface of the satellite. Let's try to get some idea of the rate of mass absorption that is likely to occur. For example, a highly conducting body will not allow much of the oncoming magnetic field to diffuse into it. So it seems likely only a small amount of the plasma will be captured by the satellite in this case. On the other hand, the satellite may be a poor conductor and hardly disturb the magnetic field (or equivalently the convection electric field). In this situation we may expect a shadow region downstream of the body, and the satellite would absorb a mass flux of order

$$(+)\rho V_c L_1 L_2 \tag{5}$$

(ρ is the plasma density). This will be a reasonable estimate for a cold plasma, but probably a lower limit for a hot plasma as there would be significant plasma motion along the field lines.

Of course the satellite could be a significant source of material if there is out-gassing or sputtering, as is the case at Io and cometary bodies. Whilst this can easily be accommodated into our model, we shall confine ourselves to the more common situation where the satellite acts as a sink of material.

Momentum Flux

In order to consider the momentum flux we need to define some directions. The cartesian coordinate system (α, β, γ) will be used - see Figure 1. The $\hat{\gamma}$ direction is aligned with $\mathbf{B}_0$, and $\hat{\beta}$ points upstream (antiparallel to $\mathbf{V}_c$). The orthogonal triad is completed by $\hat{\alpha}$ which is aligned with the background convection electric field, $\mathbf{E}_c$=-$\mathbf{V}_c \wedge \mathbf{B}_0$. From equation (2) it is clear that the conductor's $\hat{\beta}$ momentum will decrease by $L_2 I_s B_0$ per unit time. Recalling Ampère's law used above, this may be written in terms of the amplitude of the Alfvénic magnetic field ($\tilde{b}$),

$$(-)L_1 L_2 \tilde{b} B_0/\mu_0 \tag{6}$$

The negative sign means that the satellite acts as source of $\hat{\beta}$ momentum (equivalent to a sink of $-\hat{\beta}$ momentum) within the box sketched in Figure 1. If the satellite absorbs plasma at the rate given in equation (5), then there will be a further decrease in the satellite's $\hat{\beta}$ momentum of order

$$(-)\rho V_c^2 L_1 L_2 \tag{7}$$

Energy Flux

As we have already discussed, the change in satellite kinetic energy (in this situation) is zero. However, there is also another energy flux that we need to consider - namely the dissipation of electromagnetic energy in the conductor due to Joule heating. This dissipation rate represents an increase in the conductor's internal energy, and is given by the product of the conductor's volume, the electrical conductivity, and the square of the internal electric field. The electical conductivity is equal to L_2/L_1^2 times the conductance, Σ_s. The total internal electric field is reduced to $E_c(1-\varepsilon)$ as a result of charge re-distribution within the conductor. Hence the energy dissipation rate is

$$(+)2\varepsilon(1-\varepsilon)\rho V_c^2 V_A L_2^2 \tag{8}$$

To obtain this result we have expressed Σ_s in terms of ε by using equation (1), and the fact that the Alfvén conductance is related to the Alfvén speed by $\Sigma_A = 1/(\mu_0 V_A)$.

In addition to this sink of energy, the conductor may absorb plasma at the rate given by (5). If this is the case, then kinetic energy and enthalpy are removed from the plasma and turned in to satellite energy at a rate

$$(+)L_1 L_2\left[\tfrac{1}{2}\rho V_c^3 + \frac{\gamma p V_c}{(\gamma-1)}\right] \tag{9}$$

assuming that the plasma obeys an adiabatic equation of state.

This concludes our discussion of the manner in which the conductor will enter the continuity equations as a source or sink, and hence the fluxes across the inner surface. In the following sections we evaluate the contributions of the plasma disturbances to fluxes across the outer boundary.

3. PLASMA WAVES

It has been established in previous work that the Alfvén mode [*Drell et al.*, 1965] and the slow mode [*Linker et al.*, 1988] are likely to form standing wave-trains extending away from the satellite along their respective characteristics. This has been sketched in Figure 1. There will no doubt be some fast mode disturbance also, but for the present study we shall focus upon the more ducted Alfvén and slow perturbations. If it is assumed that the conducting satellite is the only source of MHD waves it follows that the waves will become seperated in space as they propagate away from the satellite. This property means that we can calculate separately for each wave the flux of mass, momentum and energy carried into the box shown in Figure 1 quite easily, if the box is made sufficiently large. For a large box we are able to perform local calculations in the regions where the wave-trains cross the surface of the box. We shall constuct our box so that all wave-trains intersect either the upper or lower faces of the surface.

The detailed derivation of the Alfvén and slow wave fields is reserved for Appendicies B and C respectively. The essential features will be described here, along with the continuity equations. Figure 2 shows the perturbed magnetic field line and streamline for the upper Alfvén wave. The wave trains make an angle θ_a with respect to the background magnetic field, and the structure is invariant in this direction. It is well known that the Poynting flux in an Alfvén wave is a second order quantity (as are the mass and momentum fluxes). For this reason we employ the nonlinear Alfvén wave solution described by *Neubauer* [1980] and *Wright and Southwood* [1987]. In this solution there is a second order parallel magnetic field and velocity perturbation. This causes the plasma streamline to move along the magnetic field in Figure 2. Figure 2*a* corresponds to field lines that pass through the conductor, while Figure 2*b* describes field lines that pass around the side of the conductor (see *Wright and Southwood* [1987] for a more complete discussion). The sense of the field aligned velocity perturbation is such that it serves to remove streamlines from the box on both upper and lower faces.

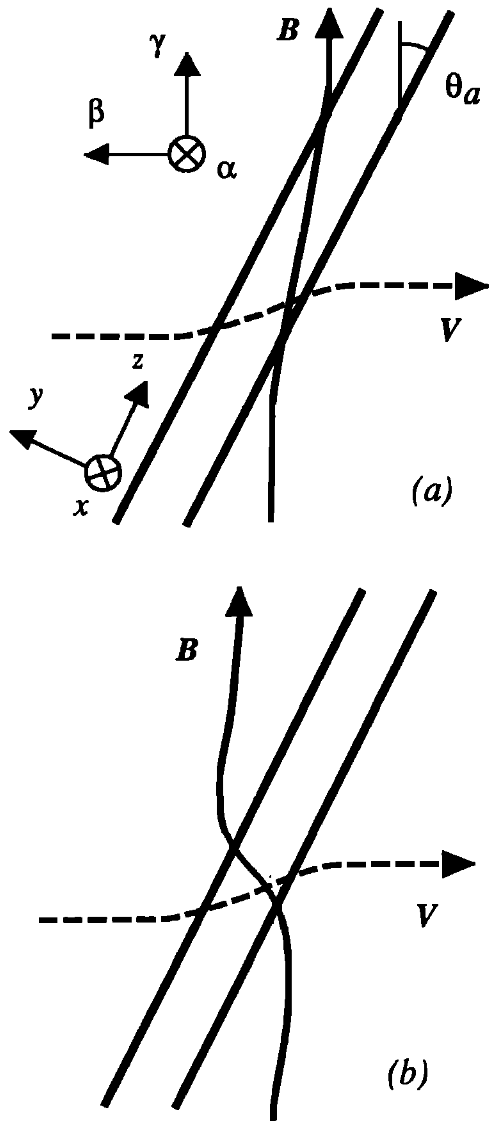

Fig. 2. The form of the magnetic field (solid line) and plasma streamlines (dashed line) when disturbed by the Alfvén wave: (Only the upper wing is shown.) The wing lies back at an angle θ_a relative to the background field direction. (*a*) The field line passes through the central portion of the wing, and would have diffused through the conductor at some earlier time. (*b*) The field line did not come in to contact with the conductor, but was pushed around the side of the conductor due to field lines like that in Figure 2*a* getting hung up at the satellite. In both cases there is a parallel velocity perturbation and this is in such a sense that it will remove plasma from the box in Figure 1 on both upper and lower faces. Also shown are the two coordinate systems (α,β,γ) and (x,y,z) employed in the text.

The slow mode model we adopt is linear since there are first order contributions to all fluxes. The slow wave-trains make an angle θ_s relative to $\mathbf{B}_0$. Due to the slower parallel propagation velocity of the slow mode relative to the Alfvén mode, θ_s is always greater than θ_a. Figure 3 shows the perturbed magnetic field lines and streamlines in the slow mode

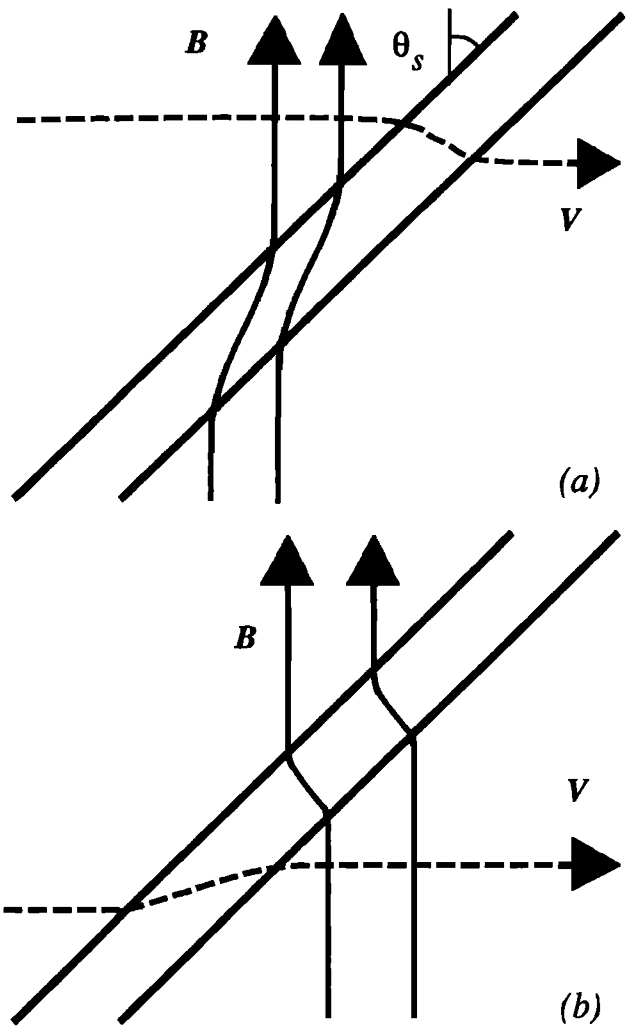

Fig. 3. The slow mode wave-trains lie downstream of the Alfvénic ones, and make an angle θ_s to $\mathbf{B}_0$. There are two solutions for the slow mode wake, and these are shown above for the upper wing: (*a*) The field pressure is enhanced, the plasma pressure depressed and there is a field-aligned flow directed toward the satellite (for both upper and lower wings). These properties can be infered from the perturbed magnetic field and streamlines. (*b*) The alternative solution is shown; the field pressure drops, the plasma pressure increases, and there is a parallel flow away from the satellite for both upper and lower wings.

wake (again for the upper face). It is shown in Appendix C that there are two possible solutions for our slow wave model corresponding to a rarefaction or compression in the plasma pressure. The former is shown in Figure 3*a* and is associated with an enhanced magnetic pressure. The depressed plasma pressure drives a field aligned flow perturbation into the box both for upper and lower wings. The alternative solution is sketched in Figure 3*b*. Here the raised plasma pressure drives the streamline out of the box (for both wings) and is consistent with a drop in magnetic field pressure. We shall see in the next section that the solution we require is the one in Figure 3*a*, and indeed such a rarefaction wave was found in the simulation performed by *Linker et al.* [1988]. The solution in Figure 3*b* (where mass is transported away from the satellite) may be of importance when considering a body that is a significant source of material.

What happens to the slow mode wave-trains in the cold plasma limit? As the plasma becomes cooler, the tilt angle θ_s of the slow mode wake approaches 90° since the propagation speed becomes very small. In the cold plasma limit the slow mode would correspond to a shadow region directly downstream of the satellite.

Mass Flux

Let us consider the continuity within the plasma volume to begin with. The familiar equation we require is

$$\frac{\partial \rho}{\partial t} + \nabla \cdot (\rho \mathbf{V}) = 0 \tag{10}$$

By working in the massive satellite's rest frame we may neglect the temporal variation of the flow. Performing a volume integral over the plasma between the inner and outer boundaries, and using Gauss' theorem we can express continuity in the form,

$$\int_{s_0} \rho \mathbf{V} \cdot d\mathbf{S} + S_{mass} = 0 \tag{11}$$

The surface integral is carried out over the outer boundary of the box (s_0), as shown in Figure 1*b*. The term S_{mass} represents any sources or sinks of mass contained within the conductor's volume - i.e. it represents the net flux across the inner boundary. For the case of a weak conductor sweeping-up background plasma, an estimate of S_{mass} is given by equation (5). Since the wave-trains pass through the upper and lower surfaces, we need only calculate the integral in equation (11) over the γ surfaces for a large box. The preceding discussion shows that the Alfvénic contribution to equation (11) will be to remove mass from the box, while the slow mode (in Figure 3*a*) will tend to return plasma. In fact one could imagine perturbation streamlines that are directed along the slow characteristics toward the satellite, and then along the Alfvénic characteristics away from the satellite. Of course, if the satellite is a source or sink of material some of these streamlines must begin or terminate at the conductor.

Momentum Flux

Continuity of plasma momentum, unlike that of mass, has three components. We may write the i^{th} component as

$$\frac{\partial(\rho V_i)}{\partial t} + \frac{\partial}{\partial x_j}\left(P_{ij} + \rho V_i V_j + \frac{B^2}{2\mu_0}\delta_{ij} - \frac{1}{\mu_0}B_i B_j\right) = 0 \tag{12}$$

and is summed over the j index. We shall assume that the pressure tensor P_{ij} is isotropic. Using a similar manipulation to before this can be written as a surface integral over the box,

$$\int_{s_0} \left(P_{ij} + \rho V_i V_j + \frac{B^2}{2\mu_0}\delta_{ij} - \frac{1}{\mu_0}B_i B_j\right) dS_j + S_{i\ mom} = 0 \tag{13}$$

$S_{i\ mom}$ represents any sources or sinks of the i^{th} component of momentum contained within the satellite volume. It is equal to the sum of equations (6) and (7) for the $\hat{\beta}$ component. Again, only the γ surfaces need be considered for a large box. To get some idea of how the waves will affect the momentum in the box consider the perturbed streamlines in Figures 2 and 3. If the field aligned flow perturbation is directed out of the box and has speed $u_{\|}$, then roughly speaking, plasma momentum is removed at a rate, per unit area, of $\rho \mathbf{V}_c u_{\|}$. (See the second term in equation (13).) Recalling that $\mathbf{V}_c$ is antiparallel to $\hat{\beta}$, this would correspond to an influx of positive $\hat{\beta}$ momentum. If $u_{\|}$ is directed into the box there would be a flux of $\hat{\beta}$ momentum out of the box (since negative $\hat{\beta}$ momentum is being brought into the box). The isotropic pressure tensor (equal to $p\delta_{ij}$) and the magnetic pressure term act in a similar manner to one another; for example, if there is a lower integrated pressure on one γ surface than on the other there will be a pressure gradient that will influence the $\hat{\gamma}$ plasma momentum. The effect of the remaining magnetic term in equation (13) is not so easy to visualize, and arises from magnetic tension. We refer the reader to Appendicies B and C where the complete momentum flux integral is evaluated for the the Alfvén and slow modes respectively. The conductor enters the continuity of momentum as a source of $\hat{\beta}$ momentum ($S_{\beta\ mom}$) due to the Lorentz force upon it (equation (6)) and any oncoming plasma that may adhere to its surface (equation (7)).

Energy Flux

The interchange of energy within a plasma between kinetic, internal and magnetic energies is expressed in the conservation of energy equation;

$$\frac{\partial}{\partial t}\left[\tfrac{1}{2}\rho V^2 + \frac{p}{\gamma - 1} + \frac{B^2}{2\mu_0}\right] + \nabla \cdot \left[\mathbf{V}\tfrac{1}{2}\rho V^2 + \frac{p}{\gamma-1}\mathbf{V} + p\mathbf{V} + \frac{\mathbf{E}_\wedge \mathbf{B}}{\mu_0}\right] = 0 \tag{14}$$

In energy equations γ denotes the polytropic index of the plasma. Equation (14) states that the rate of change of energy density in the plsama volume is balanced by a divergence in the energy flux density. The quantities in the first bracket represent the bulk kinetic energy density, the internal energy density, and the magnetic energy density. These can be identified with similar terms in the second bracket, the first of which is the flux of kinetic energy density. The second term is the flux of internal energy density, while the third term represents the rate at which work must be done to move through the gas pressure. (The sum of these two terms is the flux of enthalpy density.) The final term is the Poynting flux, and is equal to the flux of magnetic energy density ($\mathbf{E}_\wedge \mathbf{B}/2\mu_0$) plus the rate at which work must be done (per unit volume) to move through a 'magnetic pressure' of $B^2/2\mu_0$ (this is also ($\mathbf{E}_\wedge \mathbf{B}/2\mu_0$)). Thus the Poynting flux is interpreted correctly as the magnetic enthalpy flux density, rather than the magnetic energy flux density [*Siscoe*, 1982].

The energy equation (14) may be written in the alternative steady-state form

$$\int_{s_0} \left(\mathbf{V}\tfrac{1}{2}\rho V^2 + \frac{\gamma p}{\gamma - 1}\mathbf{V} + \frac{\mathbf{E}_\wedge \mathbf{B}}{\mu_0}\right) \cdot d\mathbf{S} + S_{energy} = 0 \tag{15}$$

We know that the satellite may act as a sink of electromagnetic energy (equation (8)) and also as a sink of plasma kinetic and internal energies (equation (9)) if it absorbs plasma. Indeed, S_{energy} is simply the sum of these two equations. In a steady state, this sink must be fed by a net flux of energy across the surface of the box. It is evident that waves whose parallel velocity is directed out of the box (like the Alfvén mode) will carry bulk kinetic and internal energies out of the enclosed volume, whereas an inwardly directed parallel velocity (like the slow mode solution we anticipate) will increase the bulk kinetic energy and internal energy contained within the box. The only remaining energy fluxes to discuss in equation (15) are the magnetic ones. In the Alfvén wave this points in the same sense as the other Alfvénic energy fluxes. The Poynting flux in the slow mode is second order, and can be neglected as there are first order internal and kinetic fluxes. Thus the Alfvén wave acts to remove energy from the box, while the slow mode (in Figure 3*a*) acts to bring energy into it. In equilibrium, the difference between these two rates will be equal to the sink of energy provided by the satellite.

4. DISCUSSION

In section 3 we have discussed in a qualitative fashion the mass, momentum and energy fluxes associated with the Alfvén and slow modes. The detailed wave fields and fluxes for these two modes are derived in Appendicies B and C. Using these results we shall now consider the fluxes quantitatively. Table 1 summarises the results of the continuity equations for mass, $\hat{\beta}$ momentum, and energy. (The $\hat{\alpha}$ and $\hat{\gamma}$ compoments of momentum flux are identically zero.) The terms in curly brackets are applicable when the satellite absorbs plasma at the rate given in equation (5), and should be disregarded if there is no absorption. The amplitude of the Alfvén wave velocity perturbation ($\tilde{u}_\perp$) is again expressed

TABLE 1. Contribution of the Satellite, the Alfvén Waves and the Slow Mode to the Continuity of Mass, $\hat{\beta}$ Momentum and Energy Fluxes

Origin	Mass	$\hat{\beta}$ Momentum	Energy
Satellite	0	$(-)\varepsilon\rho_0 V_c^2 L_1 L_2/M_a$	$(+)2\varepsilon(1-\varepsilon)\rho_0 V_c^3 L_2^2/M_a$
{+ absn.}	$\{(+)\rho_0 V_c L_1 L_2\}$	$\{(-)\rho_0 V_c^2 L_1 L_2\}$	$\left\{(+)L_1 L_2\left[\frac{1}{2}\rho_0 V_c^3 + \frac{\gamma p_0 V_c}{\gamma-1}\right]\right\}$
Alfvénic	$(+)\varepsilon^2\rho_0 V_c M_a A_a$	$(-)2\varepsilon^2\rho_0 V_c^2 M_a A_a$	$(+)\varepsilon^2\rho_0 V_c^3\left[\frac{5}{2}M_a + \frac{c_s^2}{V_c^2}\frac{M_a}{\gamma-1} + \frac{2}{M_a}\right]A_a$
Slow	$(-)\delta\rho_0 V_c A_s$	$(+)\delta\rho_0 V_c^2\left[1 + \frac{V_A^2}{V_c^2}\left(M_s^2 - \frac{V_c^2}{c_s^2}\right)\right]A_s$	$(-)\frac{1}{2}\delta\rho_0 V_c^3\left[1 + \frac{c_s^2}{V_c^2}\frac{1}{\gamma-1}\right]A_s$

The Alfvén and slow mode fluxes are integrated over the outer surface (s_0) shown in Figure 1. The terms in braces represent the effect of plasma absorption by the satellite. The sign convention used in front of the terms given above is as follows; fluxes out of the plasma volume (and equivalent sinks in the satellite volume) are positive, while fluxes into the plasma volume (and equivalent sources in the satellite volume) are negative. When continuity is satisfied the sum of each column is zero.

as a fraction ε of the convection velocity V_c. The slow mode velocity is predominantly along the field lines, and we expess the amplitude $\tilde{u}_{\|}$ for the upper wing as an unknown fraction $-\delta$ of the convection speed. (The negative sign is included since $u_{\|}$ is negative on the upper wing, hence δ will be positive.) The Alfvén and slow Mach numbers are given by M_a and M_s respectively, and the area of the upper/lower face of the box cut by each wave is A_a and A_s. These areas may be taken to be equal to $L_1 L_2/\cos\theta_{a,s}$ in the absence of detailed knowledge of the wake structure. The speed of sound waves in the plasma is denoted by c_s. To evaluate the size of surface integrals we simply take the product of the magnitude of the flux with the appropriate area. The sign convention used in front of the terms in Table 1 is as follows; fluxes out of the plasma volume (and equivalent sinks in the satellite volume) are positive, while fluxes into the plasma volume (and equivalent sources in the satellite volume) are negative. With this convention continuity is satisfied if the sum each of column is zero.

Several interesting features are already apparent. To begin with we shall concentrate upon the simple satellite/Alfvén wave system that has often been used in previous studies. Continuity of mass flux: The table shows how the Alfvén wave will transport mass steadily out of the box. In this simple system there is no source of mass at the conductor to balance this outflux, nor any other flow perturbation to account for the necessary displacement of streamlines downstream. In Figure 4 we have sketched the perturbed streamlines due to Alfvén waves. (We have assumed that the conductor does not act as a source or sink of matter.) From the streamlines it is evident that the mass flux out of the downstream face of the box must be less than that entering the upstream face, since the Alfvén waves have pushed some streamlines out of the upper and lower faces. We have shown this result, rather simplistically, as a shadow region downstream from the satellite. (This shadow is *not* due to plasma being absorbed by the satellite, but is entirely a consequence of the Alfvén wave disturbance.) In a warm plasma the shadow would undoubtedly distribute itself along the background field in the form of a slow (and perhaps fast) wave-train. This is, in fact, our fundemental conclusion; there must be some non-Alfvénic disturbances in the plasma if Alfvén waves are excited by the conductor. Indeed, if the satellite actually absorbs plasma the imbalance in mass continuity becomes even worse. Continuity of $\hat{\beta}$ momentum flux: The Alfvénic perturbations serve to bring a flux of $\hat{\beta}$ momentum into the box, suggesting that there is a steady sink somewhere. However, the Lorentz force on the satellite means that the conductor is a source of $\hat{\beta}$ momentum, so again the two can not balance. Once more, if there is plasma absorption, the imbalance becomes even worse. Continuity of energy flux: All of the energy fluxes in the Alfvén wave remove energy from the box, and would require a source of energy within to feed this loss. The conductor is a sink of energy (due to Joule heating), and also a sink if it absorbs plasma - so it will not balance the Alfvénic energy flux. In fact, the simple satellite/Alfvén wave system violates all three continuity equations. The conclusion being that it is not possible for such a system to exist independently of other plasma disturbances. The reason that we chose the slow mode solution in Figure 3*a*, rather than that in Figure 3*b*, is because the former will act to balance all three continuity equations. (This was also the sense of the solution found in the simulation reported by *Linker et al.* [1988].)

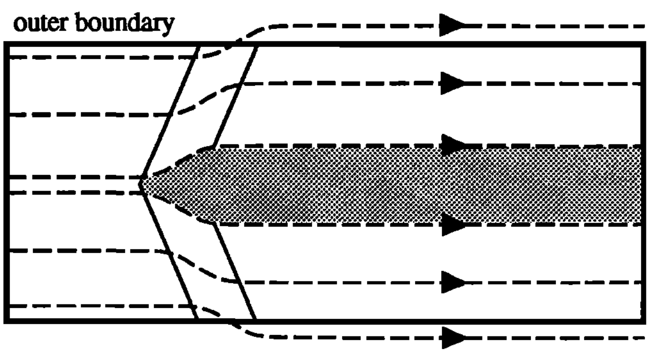

Fig. 4. The effect of purely Alfvénic disturbances upon the flow. (No plasma is absorbed by the satellite in this figure.) The Figure is sketched in a (β, γ) plane passing through the Alfvén wings. The plasma streamlines are represented by the dashed lines. The region perturbed by the Alfvén waves lies between the characteristics shown, where plasma experiences a field-aligned flow perturbation. Of the plasma entering the upstream face of the box, some is pushed out of the upper and lower faces. The result is a depleted plasma flow out of the downstream face (see the hatched region), which is a simplified manefestation of the other wave modes which are required to represent this region properly.

To test the results presented in Table 1 we shall see how well the simulation presented in Figure 4 of *Linker et al.* [1988] satisfy our continuity relations. In their model a spherical conductor was used, so we shall set $L_1 = L_2 = L$, where L is the diameter of the sphere. Also, $M_s = 1$ and $M_a = \frac{1}{2}$, implying $V_c^2/c_s^2 = \frac{6}{7}$ (see equation (C4)). If we assume that the Alfvén and slow wave-trains have a cross-section of approximately L^2, then we may take $A_a \approx L^2/\cos\theta_a$ and $A_s \approx L^2/\cos\theta_s$. Unfotunately we can not infer both ε and δ from Linker et al.'s figures. However, we can estimate δ from their Figure 4. The plasma pressure inside the slow mode wake drops by 10 – 20 percent. The amplitude of the slow mode ($\delta = -\tilde{u}_\gamma^+/V_c$) can be expessed in terms of the pressure change ($\tilde{p}_1$) by using equations (C1b) and (C3b)

$$\delta = -\left(\frac{\tilde{p}_1}{p_0}\right)\frac{M_s}{\gamma}\frac{c_s^2}{V_c^2} \tag{16}$$

This would suggest that δ lies in the range $0.07 \rightarrow 0.14$. Given δ and the three continuity equations we should be able to predict three values for ε, the amplitude of the Alfvén wave. Finding a consitent amplitude to satisfy all three continuity equations will be the critical test of our results. Before evaluating the Alfvén wave amplitude, we should point out that *Linker et al.* [1988] set the plasma velocity component normal to their conducting sphere to zero. In keeping with this we have neglected plasma absorption by the satellite, and omitted the terms in curly brackets in Table 1. In principle, we might expect the boundary conditions of *Linker et al.* [1988] to result in $\varepsilon = 1$, corresponding to a perfect conductor. However, if we assume δ to be in the range stated above, then continuity of mass flux requires $0.2 \leq \varepsilon \leq 0.4$, continuity of $\hat{\beta}$ momentum flux that $0.05 \leq \varepsilon \leq 0.15$, and continuity of energy flux that $0.1 \leq \varepsilon \leq 0.15$. We find the agreement of these independent estimates very encouraging, especially given the crudeness of our integral evaluation and slow mode model. We are unable to ascertain whether the departure from $\varepsilon = 1$ is due to details of the numerical solution, to our simplified treatment of the Alfvén and slow modes, or to our neglect of the fast mode.

The application of our work to other situations (and also an estimate of the extent to which inclusion of only lowest order Alfvén and slow mode contributions provide a reasonably self-consistent solution) can be achieved by inserting appropriate quantities into Table 1 and searching for values (ε, δ) which enable all the columns to sum to zero. However, when treating the case of a cold plasma care must be taken as the slow mode wave-train makes an increasingly large intersection (A_s) with the top and bottom surfaces. The perturbation parallel velocity of the slow mode ($\tilde{u}_{\parallel} = -\delta V_c$), on the other hand, may compensate by decreasing in amplitude. It should also be noted that in the large plasma beta limit the slow mode is no longer guided by the background field, so the present analysis and Figure 1*a* may become poor representations of the true situation.

Finally, we shall return to the original problem that motivated Drell et al., namely the 'anomalous' drag experienced by the Echo 1 satellite. The satellite was observed to be losing kinetic energy at a rate of about $\frac{1}{3}$ W, as reported by *Drell et al.* [1965]. They tried to estimate the change in kinetic energy by conservation of energy once the Alfvén wave field had been assumed. As we have already pointed out, this can only be done reliably if all of the energy fluxes are taken into account. A much surer way to estimate the drag is from the work done by the Lorentz force on the conductor (equation (3)). Using this equation the drag (viewed by a terrestrial observer) can be estimated by taking the following values from *Drell et al.* [1965]; $L_2 = 15$ m; $V_s = 7 \times 10^3$ m s^{-1}; mean $I_s \approx 0.1$ A; and $B_0 \approx 4 \times 10^{-5}$ T. Substituting these values in equation (3) suggests a drag of 0.4 W, which is close to the observed value.

5. CONCLUDING REMARKS

We have considered the equilibrium of a conducting body embedded in a steady, uniform flowing magnetised plasma. By assuming that all of the induced current within the conductor is closed in the stationary Alfvénic structure attached to the satellite, it is possible to derive the Alfvén wave field. This is done in the rest frame of a massive satellite. Such a body may be treated as a steady source of waves on MHD time scales. Some interesting features of our nonlinear Alfvén wave solution are a transport of matter away from the conductor, and an energy flux that is composed of kinetic and internal energy fluxes in addition to the Poynting flux. The general expression we provide for the Poynting flux (Appendix B) may be found to agree with those derived by other workers when the relative plsama velocity is first order.

Working in the satellite rest frame it is evident that the simple satellite/Alfvén wave system can not satisfy any of the continuity equations. In an effort to restore continuity we introduce a slow mode wake in addition to the Alfvén wake. The slow mode can go a long way toward supplying the missing fluxes. The small remaining imbalance of our new satellite/Alfvén/slow mode solution could be due to simplifications in our model. On the other hand, the discrepancy could be a real one due to our neglect of the fast mode. Whatever the cause, we have shown that it is not possible for a conductor to excite solely Alfvén waves - there must be some non-Alfvénic disturbances excited too.

Existing models have derived the wave fields in the plasma by matching boundary conditions at the surface of the conductor. Most studies have concentrated upon the Alfvén mode, but it would be interesting to look for the existence of slow or fast modes in these wave fields. It may be that these modes are not present if the boundary condition employed is only current continuity, rather than conservation of mass, momentum and energy too. However, if this is the case, caution should be exercised when considering mass, momentum and energy conservation as there are certainly non-Alfvénic plasma disturbances present.

An interesting direction to continue this work in would be the modeling of the fast mode, as this is likely to play a more important role in some stuations than in the results of *Linker et al.* [1988]. For example, studying strongly out-gassing bodies such as comets would require a large transport of material away from the body. It may be difficult to satisfy the continuity equations in this case without the fast mode.

APPENDIX A

The behaviour of the satellite in the massive limit has been discussed, when viewed from its rest frame. In this Appendix we shall consider the behaviour of an arbitrary mass satellite under the influence of electromagnetic forces. We shall also describe the evolution observed in the other natural reference frame - the plasma rest frame. It is instructive to note that, while consistent treatments can be achieved in either frame, the details of their interpretation appear different in the two frames.

Finite Mass Satellite Viewed in the Plasma Rest Frame

In this case (equation (4) not valid) the satellite is moving through the plasma and slowing down according to (2), while its kinetic energy decreases according to (3). As time passes the velocity of the conductor tends to zero, and its kinetic energy is expended as the work done moving the force $\mathbf{I}_s(t)\wedge\mathbf{B}_0$ through the displacement $\int \mathbf{V}_s(t)dt$.

Massive Satellite Viewed in the Plasma Rest Frame

This is the situation considered by *Drell et al.* [1965]. For a massive satellite $\mathbf{V}_s$ does not change significantly on the time scale that MHD waves are radiated on, and we maintain $\mathbf{V}_s(t) \approx -\mathbf{V}_c(t=0)$. The satellite expends kinetic energy at the rate given in (3), which is a finite rate, but since the satellite has 'infinite' kinetic energy (actually $\kappa \gg \frac{1}{2}L_1L_2I_sB_0$) it may dissipate this power indefinitely (compared to the MHD time scale L_1/V_c).

Finite Mass Satellite Initially at Rest

Finaly we shall consider the evolution of a finite mass satellite from the frame in which it is initiallty at rest, $\mathbf{V}_s(t=0) = 0$. In the case of a finite mass the velocity increases at the rate given in (2) and will tend to the plasma velocity, viewed from this frame. The kinetic energy increases from zero, according to (3), and tends to $\frac{1}{2}m_sV_c^2(t=0)$. Again, this is equivalent to the work done by the Lorentz force as it moves the satellite through $\int \mathbf{V}_s(t)dt$. (Note that in this frame $\mathbf{V}_s \rightarrow \mathbf{V}_c(t=0)$ and $\mathbf{I}_s \rightarrow 0$ as $t \rightarrow \infty$.) The satellite appears to be picked-up by the field, and is similar to mass pick-up in comets and in the Io wake [*Southwood and Dunlop*, 1984].

APPENDIX B

The nonlinear Alfvén wave fields and their associated fluxes are derived in this Appendix. The solution is characterized by a wave-train forming an angle θ_a to the background magnetic field. The Alfvén Mach number is given by $M_a = \tan\theta_a = V_c/V_A$ ($\mathbf{V}_A$ is the Alfvén speed). The two wave-trains propagate with velocities $\mathbf{V}^\pm = \mathbf{V}_c \pm \mathbf{V}_A$, where upper and lower signs correspond to the upper and lower faces in Figure 1. The velocity and magnetic field perturbations in an Alfvén wave satisfy the Alfvén, or Walen, relation

$$\mathbf{u}^\pm = \mp\frac{\mathbf{b}^\pm}{\sqrt{\mu_0\rho}} \quad \text{(B1)}$$

The nonlinear Alfvén wave has a parallel field and flow perturbation. These can be found by expanding the solutions of *Neubauer* [1980] and *Wright and Southwood* [1987] up to second order,

$$b_\parallel^\pm = \frac{-b_\perp^2}{2B_0}, \qquad u_\parallel^\pm = \pm\frac{u_\perp^2}{2V_A} \quad \text{(B2)}$$

The 'parallel' subscript means the component parallel to the background magnetic field. This is simply the $\hat{\gamma}$ component, i.e. $u_\parallel = (0,0,u_\gamma)$. Similarly the 'perpendicular' vector is $\mathbf{u}_\perp = (u_\alpha, u_\beta, 0)$. Another natural coordinate system for the Alfvén wave fields is a characteristic-aligned one. We shall introduce the new cartesian coordinate system (x,y,z), in which $\hat{\mathbf{z}}$ lies along the characteristic such that $\hat{\mathbf{z}}\cdot\mathbf{B}_0$ is positive and $\hat{\mathbf{x}}$ is parallel to $\hat{\alpha}$ (see Figure 2*a*). A useful relation between the two coordinate systems that we shall use is,

$$b_\beta^\pm = b_y^\pm\cos\theta_a \mp b_z^\pm\sin\theta_a \quad \text{(B3a)}$$

Additionally, a second order expansion of equation (16a) of *Wright and Southwood* yields

$$b_z^\pm = \mp b_y^\pm\tan\theta_a - \frac{b_\perp^2}{2B_0\cos\theta_a} \quad \text{(B3b)}$$

Now we are able to estimate the contribution of the Alfvén wave to the integrals (11), (13) and (15). These estimates will be found by taking the product of the appropriate perturbation amplitude, e.g. $\tilde{u}_\parallel$, with a representative area of intersection of the wing with the outer surface s_0, e.g., $A_a \approx O(L_1L_2/\cos\theta_a)$. Only terms up to and including second order will be retained in these calculations.

Mass Flux

The mass flux integral is only sensitive to the parallel velocity (B2) if the Alfvén waves exit via the upper and lower faces in Figure 1. There velocities are directed out of the box for both wings, and will make a contribution to the mass flux integral (equation (11)) over the outer surface (s_0) of order

$$2\rho_0\tilde{u}_\parallel A_a \equiv (+)\rho_0 A_a\frac{\tilde{u}_\perp^2}{V_A} \quad \text{(B4)}$$

where A_a is the area of the upper face associated with the Alfvén wave. (To obtain the entry in Table 1 we have used the definition of the Alfvén Mach number and $\varepsilon \approx \tilde{u}_\perp/V_c$.)

Momentum Flux

The properties of Alfvén waves outlined above can be used to show that the $\hat{\alpha}$ and $\hat{\gamma}$ momentum integrals (13) are zero when summed over both wings. The $\hat{\beta}$ component is nonzero, and takes the form

$$-\int\left(\rho V_c u_\gamma + \frac{b_\beta B_0}{\mu_0}\right)\hat{\gamma}\cdot d\mathbf{S} \quad \text{(B5)}$$

The first term is clearly second order, since $u_\gamma \equiv u_\parallel$ and is found from equation (B2). The second term may be written (using B3)

$$\frac{b_\beta^\pm B_0}{\mu_0} = \frac{B_0}{\mu_0}\left[b_y^\pm(\cos\theta_a + \tan\theta_a\sin\theta_a) \pm \frac{b_\perp^2\tan\theta_a}{2B_0}\right] \quad \text{(B6)}$$

The linear part (in $b_y^\pm$) integrates to zero on each surface identically for a wave of finite cross-section due to $\nabla\cdot\mathbf{b} = 0$. This can be seen qualitatively from Figure 2; note how the main b_y perturbation for field lines that have passed through the conductor (2*a*), and for those that are pushed around the side of the conductor have opposite senses. As a result, integrating b_y with respect to α across the wave cross section (at any β) yields zero. (See Figure 2 of *Wright* [1987] for a more complete picture of b_y.) This property can be proven rigorously by considering the perturbation field lines (b_x, b_y). For a wave of finite cross-section these perturbation field lines must be self-closing, since the structure is invariant in z. Thus we may write these field components in terms of a 'flux function', ψ, (e.g., equation (6) of *Wright* [1987]), in which case $b_y = -\partial\psi/\partial\alpha$. (We have used the fact that $x \equiv \alpha$.) Now, integrating b_y with respect to α becomes $-\int d\psi$. Since ψ is constant on a field line (b_x, b_y), the integral, when performed across closed loops of flux, will be zero at all β values. Summing the remaining second order terms from (B5) and (B6) over both surfaces we have $-(\rho A_a V_c\tilde{u}_\perp^2/V_A + A_a\tan\theta_a\tilde{b}_\perp^2/\mu_0)$ which may be manipulated into the simpler form

$$(-)2\rho\tilde{u}_\perp^2 M_a A_a \quad \text{(B7)}$$

Energy Flux

The only energy flux we need to consider for the integral (15) is the component parallel to $\mathbf{B}_0$. We shall begin with the Poynting flux, and make use of the nonlinear expression derived by *Wright* [1987] (his equation 14). The scalar product of this equation with $\hat{\gamma}$ yields the parallel Poynting flux $(S_\parallel^\pm)$

$$\mu_0 S_\parallel^\pm = -(\mathbf{V}^\pm\cdot\mathbf{b}^\pm)B_0 - (\mathbf{V}^\pm\cdot\mathbf{B})b_\parallel^\pm \quad \text{(B8)}$$

This expession has not been approximated. To proceed further we recall that in our model $\mathbf{V}_c\cdot\mathbf{B}_0 = 0$, and (B8) reduces to the simpler form

$$\mu_0 S_\parallel^\pm = \mp V_A B_0(b_\parallel^\pm + b_z^\pm/\cos\theta_a) \quad \text{(B9)}$$

Employing the second order approximations for $b_\parallel^\pm$ and $b_z^\pm$ we arrive at the final equation for the Poynting flux,

$$\mu_0 S_\parallel^\pm = V_A B_0 b_y^\pm\frac{\tan\theta_a}{\cos\theta_a} \pm V_A b_\perp^2(1+\tan^2\theta_a) \quad \text{(B10)}$$

The linear term in $b_y^\pm$ again integrates to zero exactly on each surface leaving a net second order Poynting flux. The other energy fluxes stem from internal and kinetic energies.

Taking the $\hat{\gamma}$ component of these is trivial, and we find that the total field-aligned energy flux is

$$\frac{1}{2}\rho V_c^2 u_{\parallel}^{\pm} + u_{\parallel}^{\pm}\frac{\gamma p}{\gamma - 1} + S_{\parallel}^{\pm} \tag{B11}$$

It is interesting to compare this result with those of other workers. This is done most clearly by allowing the relative flow speed V_c to be first order and considering the cold plasma limit (cf. *Barnett and Olbert* [1986]). In this case the kinetic energy term is fourth order and the internal energy is neglected. The integrated Poynting flux (B10) is then composed of a fourth order element and a second order one which is equal to $S_{\parallel}^{\pm} = \pm V_A b_{\perp}^2/\mu_0$. When this is multiplied by a representative area (e.g. the cross section of the wing) we find general agreement with all previous studies except for *Dobrowolny and Veltri* [1986], whose expression is less by a factor of M_a^2. (See *Estes* [1988] for further discussion.)

When the total energy flux (B11) is integrated over the intersection of both wings with the outer surface (s_0 - see Figure 1*a*) we find, to lowest order

$$(+)\rho V_c \tilde{u}_{\perp}^2 A_a \left[\frac{5M_a}{2} + \frac{c_s^2}{V_c^2}\frac{M_a}{\gamma - 1} + \frac{2}{M_a}\right] \tag{B12}$$

APPENDIX C

In this Appendix we derive the fields and fluxes associated with a standing slow mode wave. Unlike the Alfvén mode, there are first order contributions to all continuity equations, so we need only consider a linear model. We adopt a steady-state one-dimensional model, so we are really calculating the fluxes per unit length of a section of the wing. The one dimensional model is sketched in Figure 5 and is invariant along the characteristics and in the $\hat{\alpha}$ direction. This property relies upon the guided nature of slow mode wave propagation, and is satisfied best in the low plasma β limit. Only the upper wing is shown in Figure 5, and the relationship to the lower wing is discussed later. The wave vector **k** lies in the (β, γ) plane and is perpendicular to lines of constant phase. Thus **k** is perpendicular to the group velocity. The wing is inclined at an angle θ_s to the background field. The slow Mach number is given by $M_s = |\tan\theta_s|$, and $T = \tan\theta_s$ is positive on the upper wing and negative on the lower.

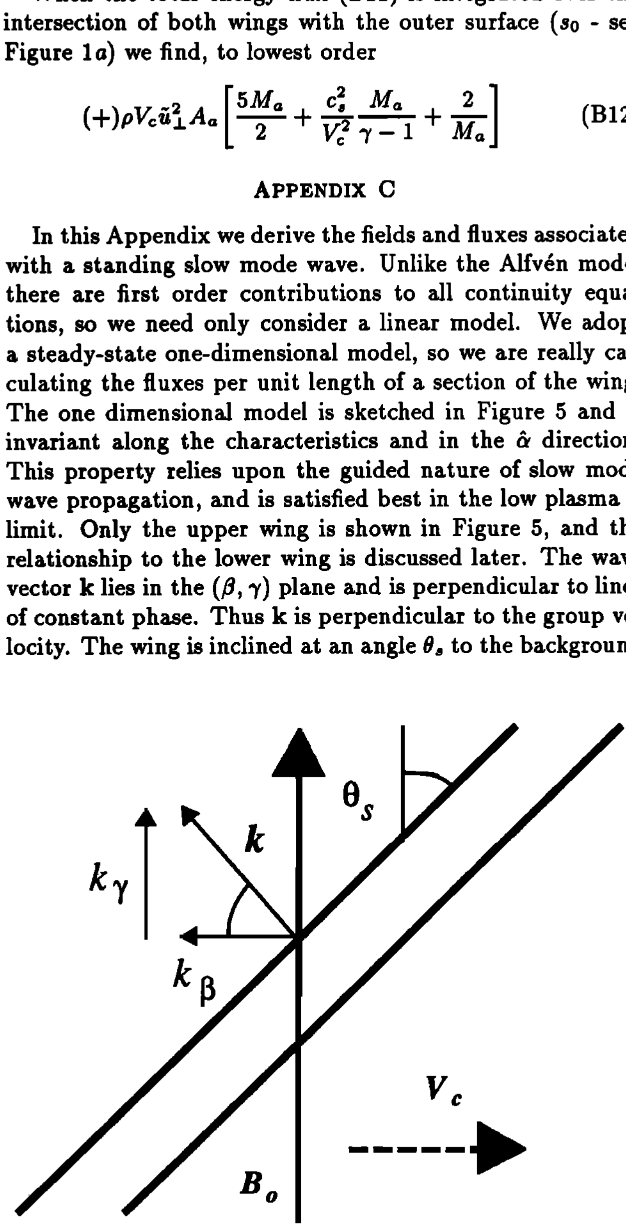

Fig. 5. A sketch of the geometry of the one-dimensional slow mode modeled in Appendix C. The characteristics coincide with surfaces of constant phase, to which the wave vector **k** is perpendicular. Only the upper wing is shown.

Setting the background field and flow to be $(0, 0, B_0)$ and $(0, -V_c, 0)$ respectively and assuming all perturbed quantities $(\rho_1, p_1, \mathbf{u}, \mathbf{b})$ vary as $e^{i\mathbf{k}\cdot\mathbf{r}}$, we may write the linearized steady-state MHD equations as

$$-k_\beta V_c \rho_1 + \rho_0(k_\beta u_\beta + k_\gamma u_\gamma) = 0 \tag{C1a}$$

$$p_1 = \rho_1 \frac{\gamma p_0}{\rho_0} \tag{C1b}$$

$$-\rho_0 k_\beta V_c \mathbf{u} = \frac{\mathbf{k}\wedge\mathbf{b}}{\mu_0}\wedge\mathbf{B}_0 - \mathbf{k}p_1 \tag{C1c}$$

$$k_\gamma B_0 \mathbf{u} + k_\beta V_c \mathbf{b} - (k_\beta u_\beta + k_\gamma u_\gamma)\mathbf{B}_0 = 0 \tag{C1d}$$

$$k_\beta b_\beta + k_\gamma b_\gamma = 0 \tag{C1e}$$

The equations are continuity of matter, isentropic equation, momentum equation, induction equation (incorporating the idealized Ohm's law), and solenoidal magnetic field condition. Subscripts 0 and 1 denote background and perturbed quantities respectively. To begin with consider the equations governing b_α and u_α. (See the $\hat{\alpha}$ components of (C1*c*) and (C1*d*).) These quantities become decoupled from the others and obey the wave equation

$$\rho_0 V_c^2 \begin{pmatrix} b_\alpha \\ u_\alpha \end{pmatrix} = \frac{B_0^2 T^2}{\mu_0}\begin{pmatrix} b_\alpha \\ u_\alpha \end{pmatrix} \tag{C2}$$

This equation is satisfied when $T^2 = V_c^2/V_A^2$ or when (b_α, u_α)=0. The former condition requires that the wing be tilted back in keeping with the Alfvén Mach number. This would correspond the Alfvén solution, which we are not interested in here. Hence we conclude that in a slow mode wake like that in Figure 4, the $\hat{\alpha}$ components of field and flow must be zero.

Equation (C1*e*) states that there is no magnetic field perturbation normal to the surfaces of constant phase, i.e., $(b_\beta = -Tb_\gamma)$. The geometry of the system also relates the components of the wave vector to each other, $k_\gamma = Tk_\beta$. Using these relations we can rewrite the equations and eliminate the b_β and k_γ dependence. When this is done the $\hat{\beta}$ and $\hat{\gamma}$ components of the induction equation become degenerate, and we are left with five independent equations for the five quantities $(\rho_1, p_1, u_\beta, u_\gamma, b_\gamma)$. To proceed further we shall expess all of these quantities in terms of only one parameter, say u_γ. The $\hat{\gamma}$ component of the momentum equation yields

$$p_1 = \frac{\rho_0 V_c}{T} u_\gamma \tag{C3a}$$

The isentropic relation and the above result give

$$\rho_1 = \frac{\rho_0^2 V_c}{\gamma p_0 T} u_\gamma \tag{C3b}$$

Continuity of mass and (C3*b*) relate u_β and u_γ

$$u_\beta = \left[\frac{\rho_0 V_c^2}{\gamma p_0 T} - T\right] u_\gamma \tag{C3c}$$

Finally, the parallel field perturbation is found in terms of u_γ from the $\hat{\beta}$ component of the induction equation and (C3*c*)

$$b_\gamma = \frac{B_0}{V_c}\left[\frac{\rho_0 V_c^2}{\gamma p_0 T} - T\right] u_\gamma \qquad (C3d)$$

The only equation we have not used is the $\hat{\beta}$ component of the momentum equation. If we substitute the above exprssions in to this equation, we find a necessary condition for non-trivial solutions (analagous to the dispersion relation in the plasma rest frame);

$$\left[\frac{V_A^2}{V_c^2}(1+T^2)\left[\frac{V_c^2}{c_s^2} - T^2\right] - \left[\frac{V_c^2}{c_s^2} - T^2\right] + 1\right] u_\gamma = 0 \quad (C4)$$

This relation implies that either $u_\gamma = 0$ (in which case there is a trivial solution with no perturbation) or the large square bracket must be zero. The latter condition defines specific values of T in terms of the three propagation speeds V_c, V_A and c_s. This result is, not surprisingly, equivalent to making use of the dispersion relation (in the plasma rest frame) and requiring that the phase speed be of magnitude $\hat{\mathbf{k}} \cdot \mathbf{V}_c$. Again, this will define special propagation angles. When this condition is satisfied the (Doppler-shifted) waves will appear stationary in the rest frame of the satellite.

Now let us calculate the transport across the outer surface (s_0) of mass, momentum and energy for a single wing.

Mass Flux

The slow mode contribution to the mass flux integral (11) for a single wing can be written to first order as

$$(\pm)\int \rho_0 u_\gamma d\beta \qquad (C5)$$

This is the mass flux per unit length in α at the outer surface (s_0). The upper and lower signs correspond to the upper and lower wings, respectively.

Momentum Flux

The $\hat{\alpha}$ component of the momentum flux integral (13) is zero because both (b_α, u_α) are zero in our solution. The $\hat{\beta}$ component is nonzero, and has a value per unit length of

$$(\pm)\int (-\rho_0 V_c u_\gamma - \frac{b_\beta B_0}{\mu_0}) d\beta \qquad (C6)$$

The $\hat{\gamma}$ component per unit α length is also nonzero, and is equal to

$$(\pm)\int (p_1 - \frac{b_\gamma B_0}{\mu_0}) d\beta \qquad (C7)$$

Energy Flux

The first order integrated energy flux (per unit α length) is found to be

$$(\pm)\int (\tfrac{1}{2}\rho_0 V_c^2 u_\gamma + \frac{\gamma p_0}{\gamma - 1} u_\gamma) d\beta \qquad (C8)$$

Note that the parallel Poynting flux is a second order quantity, and has been neglected.

In order to relate the four integrals given above, describing our one-dimensional model, to the two dimensional wave-trains shown in Figure 1 some approximations are necessary. It is interesting to construct a smooth, well-behaved variation in β for the perturbation velocity u_γ as a Fourier series in $\mathbf{k}$. Since the relations (C3) have no $\mathbf{k}$ dependence, the relative sizes of coefficients in such a series will be the same for all perturbed quantities. Hence the variation in β of all perturbations will be identical. For simplicity we shall approximate the two dimensional cross-section as having dimensions α_0 and β_0, where $A_s \approx \alpha_0\beta_0$. We need to multiply our fluxes per unit α length by α_0 to estimate the contribution from a two dimensional wave-train. Hence the two dimensional integral of, say, u_γ would be approximated by $\alpha_0 \int u_\gamma d\beta \approx \frac{1}{2}\alpha_0\beta_0\tilde{u}_\gamma \equiv \frac{1}{2}A_s\tilde{u}_\gamma$. (We have introduced a factor of a half since $\tilde{u}_\gamma$ represents the maximum u_γ perturbation in the slow mode wave, not the mean.)

This enables us to calculate the net fluxes for each wing. The only remaining question is the relationship between the upper and lower wing. Probably the most natural choice would be for both wings to experience the same pressure change. Inspection of (C3), and noting that $T^- = -T^+$, reveals the following symmetries $(p_1^+, \rho_1^+, u_\beta^+, u_\gamma^+, b_\beta^+, b_\gamma^+) = (p_1^-, \rho_1^-, u_\beta^-, -u_\gamma^-, -b_\beta^-, b_\gamma^-)$, so only u_γ and b_β change phase. With this symmetry both wings transport plasma either toward or away from the satellite, and the $\hat{\gamma}$ momentum fluxes from upper and lower wings cancel with one another. In this case we are left with the following mass, $\hat{\beta}$ momentum and energy fluxes summed over both wings,

$$(+)\rho_0\tilde{u}_\gamma^+ A_s \qquad (C9a)$$

$$(-)A_s\left(\rho_0 V_c \tilde{u}_\gamma^+ + \frac{B_0\tilde{b}_\beta^+}{\mu_0}\right) \qquad (C9b)$$

$$(+)A_s\left(\tfrac{1}{2}\rho_0 V_c^2\tilde{u}_\gamma^+ + \frac{\gamma p_0}{\gamma - 1}\tilde{u}_\gamma^+\right) \qquad (C9c)$$

This solution would correspond to a symmetric absorption or out-gassing (depending upon the sign of u_γ^+), and is the one we adopt in Table 1. (In order to obtain the entries in Table 1 we have introduced a dimensionless slow mode amplitude, $\delta = -\tilde{u}_\gamma^+/V_c$, and $\tilde{b}_\beta^+$ is proportional to $\tilde{u}_\gamma^+$ via (C3d).) The alternative solution is $(p_1^+, \rho_1^+, u_\beta^+, u_\gamma^+, b_\beta^+, b_\gamma^+) = (-p_1^-, -\rho_1^-, -u_\beta^-, u_\gamma^-, b_\beta^-, -b_\gamma^-)$, in which case the pressure drops in one wing and rises in the other. The parallel flow is the same in both wings and would correspond to plasma entering the box through one face and leaving it through the other. It is difficult to imagine such a disturbance occuring naturally, but such a system could probably be produced by an artificial satellite that pumps plasma from above it to below, along the magnetic field direction. If this were done, and the two wings were of the same magnitude, summing the integrals (C5)-(C8) over both wings produces no net flux of mass, $\hat{\beta}$ momentum or energy into the box. Not surprisingly there is a net $\hat{\gamma}$ momentum flux, and this is equal to $A_s(\tilde{p}_1^+ - B_0\tilde{b}_\gamma^+/\mu_0)$.

Acknowledgments. This work was carried out while A.N.W. was a SERC Fellow and SERC Research Assistant.

The editor thanks D. J. Donohue and another referee for their assistance in evaluating this paper.

REFERENCES

Acuña, M. H., F. M. Neubauer, N. F. Ness, Standing Alfvén wave current system at Io: Voyager 1 observations, *J. Geophys. Res., 86*, 8513, 1981.

Barnett, A. S., In situ measurements of the plasma bulk velocity near the Io flux tube, *J. Geophys. Res., 91*, 3011, 1986.

Barnett, A., and S. Olbert, Radiation of plasma waves by a conducting body moving through a magnetized plasma, *J. Geophys. Res.*, *91*, 10117, 1986.

Belcastro, V., P. Veltri, and M. Dobrowolny, Radiation from long conducting tethers in the near-earth environment, *Nuovo Cimento*, *5C*, 536, 1982.

Belcher, J. W., C. K. Goertz, J. D. Sullivan, and M. H. Acuña, Plasma observations of the Alfvén wave generated by Io, *J. Geophys. Res.*, *86*, 8508, 1981.

Boyd, T. J. M., and J. J. Sanderson, *Plasma Dynamics*, Nelson, London, 1969.

Chu, C. K., and R. A. Gross, Alfvén waves and induction drag on long cylindrical satellites, *AIAA J.*, *4*, 2209, 1966.

Dobrowolny, M., and P. Veltri, Structure of Alfvén wings associated with a conductor moving through a magnetoplsama, *Astron. Astrophys.*, *167*, 179, 1986.

Drell, S. D., H. M. Foley, and M. A. Ruderman, Drag and propulsion of large satellites in the ionosphere, *J. Geophys. Res.*, *70*, 3131, 1965.

Estes, R. D., Alfvén waves from an electrodynamic Tethered Satellite System, *J. Geophys. Res.*, *93*, 945, 1988.

Goertz, C. K., and P. A. Deift, Io's interaction with the magnetosphere, *Planet. Space Sci.*, *21*, 1399, 1973.

Goldreich, P., and D. Lynden-Bell, Io, a Jovian unipolar inductor, *Astrophys. J.*, *156*, 59, 1969.

Hastings, D. E., A. Barnett, and S. Olbert, Radiation from large space structures in low Earth orbit with induced alternating currents, *J. Geophys. Res.*, *93*, 1945, 1988.

Linker, J. A., M. G. Kivelson, and R. J. Walker, A MHD simulation of plasma flow past Io: Alfvén and slow mode perturbations, *Geophys. Res. Lett.*, *15*, 1311, 1988.

Neubauer, F. M., Nonlinear Standing Alfvén wave current system at Io: Theory, *J. Geophys. Res.*, *85*, 1171, 1980.

Rasmussen, C. E., and P. M. Banks, Theory of the electrodynamic tether, *Adv. Space Res.*, *8*, 1,203, 1988.

Rasmussen, C. E., P. M. Banks, and K. J. Harker, The excitation of plsama waves by a current source moving in a magnetized plasma: The MHD approximation, *J. Geophys. Res.*, *90*, 505, 1985.

Siscoe, G. L., Solar system magnetohydrodynamics, in *Proceedings of the 1982 Boston College Theory Institute in Solar-Terrestrial Physics*, edited by R. L. Carovillano and J. M. Forbes, D. Reidel, Hingham, Mass., 1982.

Southwood, D. J., and M. W. Dunlop, Mass pickup in sub-Alfvénic plasma flow: A case study for Io, *Planet. Space Sci.*, *32*, 1079, 1984.

Southwood, D. J., M. G. Kivelson, R. J. Walker, and J. A. Slavin, Io and its plasma environment, *J. Geophys. Res.*, *85*, 5959, 1980.

Wolf-Gladrow, D. A., F. M. Neubauer, and M. Lussem, Io's interaction with the plasma torus: A self-consistent model, *J. Geophys. Res.*, *92*, 9949, 1987.

Wright, A. N., The structure of ULF waves produced by a Tethered Satellite System, *Astron. Astrophys.*, *186*, 354, 1987.

Wright, A. N., and D. J. Southwood, Stationary Alfvénic Structures, *J. Geophys. Res.*, *92*, 1167, 1987.

S. Schwartz and A. Wright, Astronomy Unit, School of Mathematical Sciences, Queen Mary and Westfield College, Mile End Road, London E1 4NS, England.

(Received September 5, 1989;
revised November 22, 1989;
accepted December 13, 1989.)